Fisica 2
Ingegneria Industriale

Introduzione al corso

Outline

- Il docente.
- Argomenti del corso.
- Materiale di studio.
- Modalità di esame.
- Avvertenze e “strategie”.

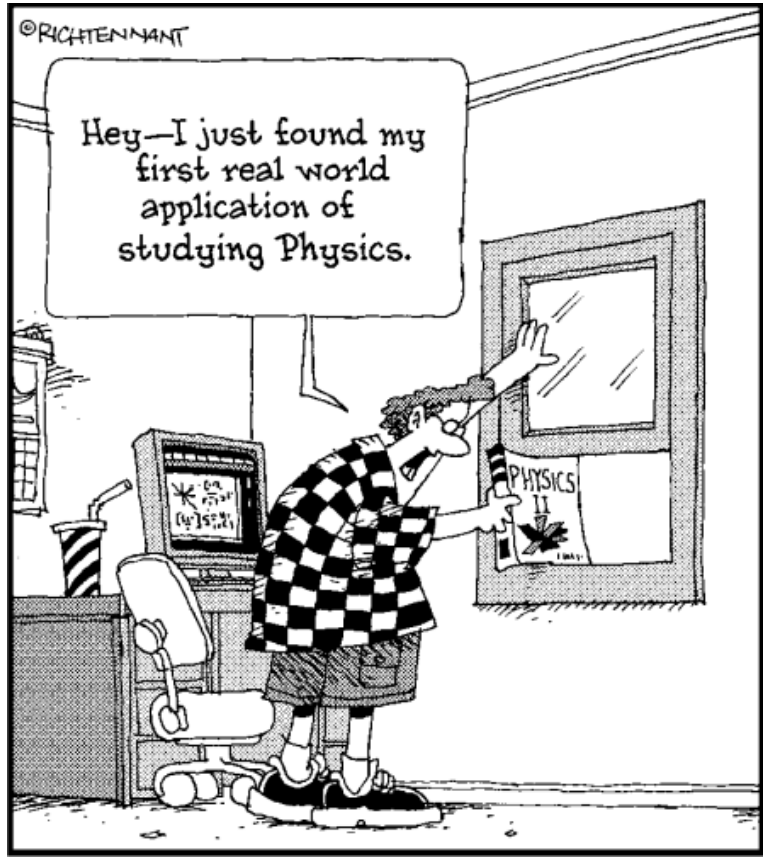

Il docente

Alberto Quaranta

Dipartimento di Ingegneria Industriale (DII)

Ufficio: Povo2, piano 0

Alberto.Quaranta@unitn.it

Altri corsi: Physics of Materials

(I anno LM ME)

Attività di ricerca

Rivelatori di radiazione scintillanti

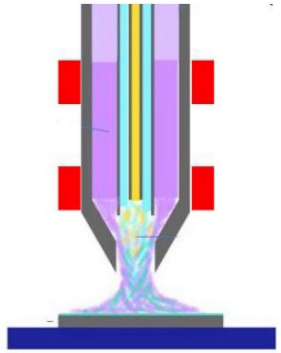

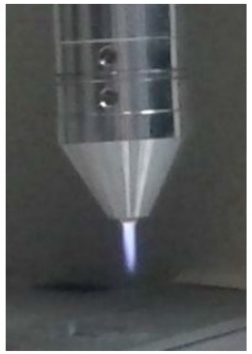

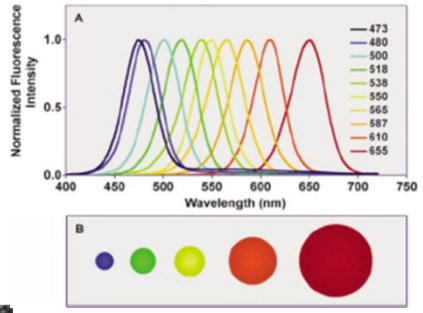

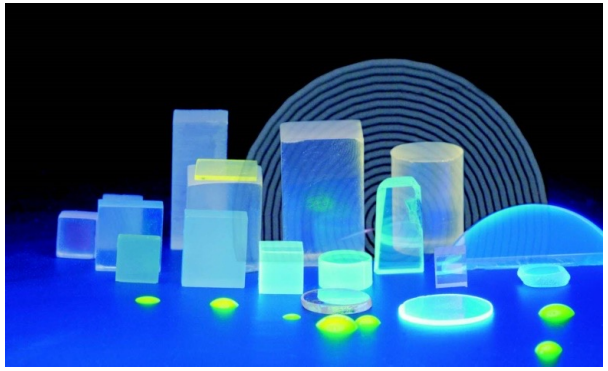

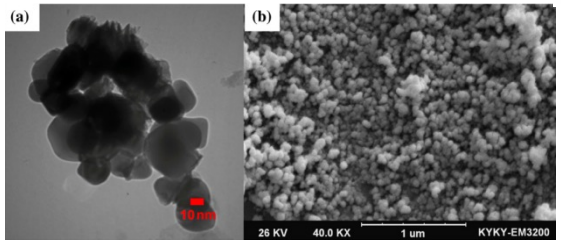

Produzione di nanomateriali con torcia al plasma

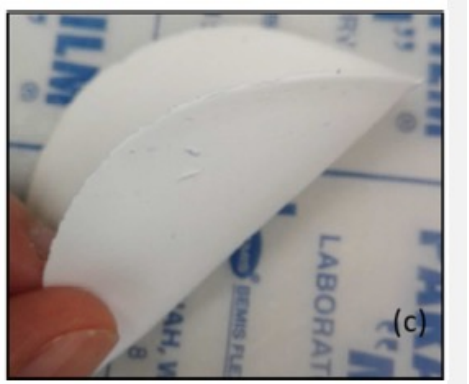

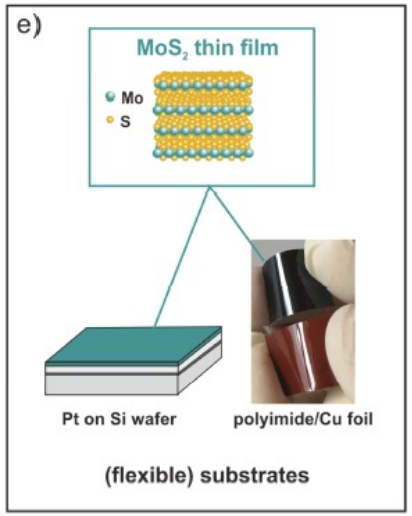

Sensori e biosensori flessibili e biocompatibili.

INFN
Istituto Nazionale di Fisica Nucleare

CSN5
Ricerca
Tecnologica

TIFPA
Trento Institute for Fundamental Physics and Applications

Nuclear Instruments and Methods in Physics Research B 96 (1995) 382–386

ELSEVIER

NIM B
Beam Interactions with Materials & Atoms

Irradiation-induced Ag-colloid formation in ion-exchanged soda-lime glass

F. Caccavale [a,*], G. De Marchi [a], F. Gonella [a], P. Mazzoldi [a], C. Meneghini [a], A. Quaranta [a], G.W. Arnold [a], G. Battaglin [b], G. Mattei [c]

[a] Unità INFM, Dipartimento di Fisica, Via Marzolo 8, 35131 Padova, Italy
[b] Unità INFM, Dipartimento di Chimica Fisica, Calle Larga S. Marta 2137, 30123 Venezia, Italy
[c] LaMEI, Area CNR, Bologna, Italy

RIVISTA DEL NUOVO CIMENTO Vol. 36, N. 9 2013
DOI 10.1393/ncr/i2013-10092-1

Ion exchange process: History, evolution and applications

P. Mazzoldi(1), S. Carturan(1), A. Quaranta(2), C. Sada(1) and V. M. Sglavo(2)

(1) Physics and Astronomy Department, University of Padova
Via Marzolo 8, Padova, Italy
(2) Department of Industrial Engineering, University of Trento
Via Mesiano 77, Trento, Italy

RESEARCH ARTICLE

ADVANCED MATERIALS INTERFACES
www.advmatinterfaces.de

Plasma-Assisted Deposition of Silk Fibroin on Different Surfaces

Artem Arkhangelskiy, Devid Maniglio, Alessio Bucciarelli, Vamsi K. Yadavalli, and Alberto Quaranta*

Optical and radioluminescence properties of ZnO:Zn as a function of reduction degree and treatment temperature

Cite as: J. Appl. Phys. **130**, 085104 (2021); doi: 10.1063/5.0057816
Submitted: 25 May 2021 · Accepted: 12 August 2021 ·
Published Online: 25 August 2021

View Online Export Citation CrossMark

M. Favaro,[1,2,a)] R. Ceccato,[1] S. Dirè,[1] E. Callone,[1] and A. Quaranta[1,2]

AFFILIATIONS

[1]Department of Industrial Engineering, University of Trento, Via Sommarive 9, I-38123 Povo, Trento, Italy
[2]INFN–TIFPA, Via Sommarive 14, I-38123 Povo, Trento, Italy

[a)]Author to whom correspondence should be addressed: matteo.favaro@unitn.it

sensors MDPI

Review

MoS_2 Based Photodetectors: A Review

Alberto Taffelli *, Sandra Dirè, Alberto Quaranta and Lucio Pancheri

Department of Industrial Engineering, University of Trento, Via Sommarive 9, 38123 Trento, Italy; sandra.dire@unitn.it (S.D.); alberto.quaranta@unitn.it (A.Q.); lucio.pancheri@unitn.it (L.P.)
* Correspondence: alberto.taffelli@unitn.it

Abstract: Photodetectors based on transition metal dichalcogenides (TMDs) have been widely reported in the literature and molybdenum disulfide (MoS_2) has been the most extensively explored for photodetection applications. The properties of MoS_2, such as direct band gap transition in low dimensional structures, strong light–matter interaction and good carrier mobility, combined with the possibility of fabricating thin MoS_2 films, have attracted interest for this material in the field of optoelectronics. In this work, MoS2-based photodetectors are reviewed in terms of their main performance metrics, namely responsivity, detectivity, response time and dark current. Although neat MoS2-based detectors already show remarkable characteristics in the visible spectral range, MoS_2 can be advantageously coupled with other materials to further improve the detector performance Nanoparticles (NPs) and quantum dots (QDs) have been exploited in combination with MoS_2 to boost the response of the devices in the near ultraviolet (NUV) and infrared (IR) spectral range. Moreover, heterostructures with different materials (e.g., other TMDs, Graphene) can speed up the response of the photodetectors through the creation of built-in electric fields and the faster transport of charge carriers. Finally, in order to enhance the stability of the devices, perovskites have been exploited both as passivation layers and as electron reservoirs.

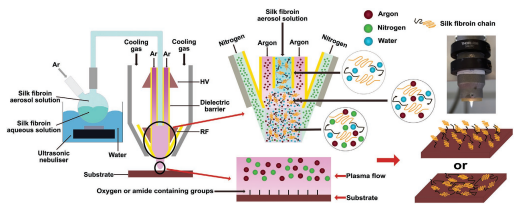

Figure 1. Schematic illustration of the deposition process: silk fibroin solution is vaporized using an ultrasonic nebulizer. The aerosol is injected into the plasma torch gas line, followed by plasma modification of the surface and deposition. Details of the process are presented in the experimental section.

on different materials, glass, PET, PDMS, and Ti6Al4V alloy were used as model substrates. Glass was used as a reference material due to insulation properties and smooth surface, while Ti6Al4V alloy was chosen as a biocompatible alloy and conductive material. PDMS and PET were chosen as polymeric materials (elastomeric and thermoplastic, respectively).

Plasma deposition of the silk fibroin results from the combination of different processes. Plasma sputtering (cleaning) of the substrate, which occurs when excited species generated from an inert gas (Ar) collides with the solid. This process not only cleans, but also sterilizes the surface. Further, during sputtering, the excited species react with the substrate surface and induce functionalization with oxygen and amide-containing groups.[35] In the plasma polymerization of silk fibroin, two simultaneous competitive processes take place. In the first phase silk fibroin is deposited on the substrate then the etching action of plasma starts to erode the formed film. Only when the deposition is predominant over etching, the thickness growth is promoted. We also hypothesize that during deposition, plasma may affect the silk-fibroin secondary structure due to the presence of free argon and N_2/O_2. Initially, the silk fibroin aerosol solution is affected by argon plasma inside the plasma gas line, changing the secondary structure and charge of fibroin chains. Then this plasma flows with the fibroin aerosol solution mixed with nitrogen (cooling gas) and is deposited on the substrate (**Figure 1**). We assume that during all steps of deposition, dehydration of the structure occurs because of the use of a dry inert atmosphere. Moreover, plasma continues to influence the already deposited layer also during deposition. Depending on the substrate and presence of already deposited layers, silk fibroin can attach and orient differently because of the continuous change at the surface and the reactive species distribution.

2.1. Optical Images of Silk Fibroin Coatings

The coatings obtained on glass, PET, PDMS, and Ti6Al4V can be observed in **Figure 2**. Deposition parameters were kept the same for all materials: power 10 W, the distance between substrate and plasma torch ≈6 mm, speed of the torch ~ 100 mm min^{-1}. Low power was set in order to reduce the influence on the etching mechanism. 10 W power is the lowest power limit to maintain a stable plasma plume. It is worth noticing that the plasma deposited silk fibroin stripes are homogeneous on all substrates with a width around 1 cm, which corresponds to the diameter of the region irradiated by the plasma plume. While the deposition on flat substrates was obtained with ease, this technique can also be applied to more complex geometries. In order to test the deposition capability on a non-planar surface, a Ti6Al4V cylindrical pin was put in rotation and exposed to the plasma torch (Figure 2d). Due to the presence of free charge carriers, plasma is electrically conductive[36] and exhibits different behavior on conductive or non-conductive substrates. On the Ti6Al4V surface, the current induced by plasma flows through the sample inducing zero charge accumulation on the top of the surface. In contrast, on insulating substrates (glass, PET, PDMS), the charge can accumulate on the top of the surface.

In order to visualize the silk fibroin on the transparent surfaces, the protein was stained using crystal violet which provides good contrast, allowing easier observation. Close-ups of these surfaces using optical microscopy are shown in the Supporting Information (Figure S1, Supporting Information). Samples were stretched and bent in order to observe the preliminary strength of adhesion. PDMS and PET samples (Figure 2a,b) show uniform coatings with no significant cracks or delamination. A slight difference in morphology can be explained by the effect of plasma or different optical properties of materials. For determining the mechanism of building-up of the silk fibroin layers, an SEM cross-section image was used, as shown in **Figure 3a**, with the sample obtained using 80 runs (resulting in a film thickness of about 6 µm). The homogeneous and uniform structure of the films is clearly observed, showing that each pass does not create growth through a layered structure. This has implications in the homogeneity and strength of the deposited bioactive film on the substrate.

© 2021 The Authors. Advanced Materials Interfaces published by Wiley-VCH GmbH

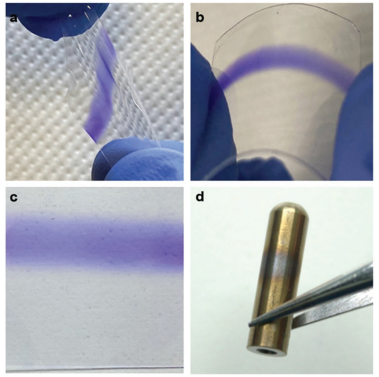

Figure 2. Images of coated samples on a) PDMS, b) PET, c) glass, and d) Ti6Al4V cylindrical pin. Blue coloration is due to the crystal violet solution.

One of the most promising applications of plasma deposited silk fibroin is in the surface modification of complex, non-planar surfaces. For instance, a screw with multiple threads and crevices, can make uniform deposition via traditional methods challenging. While a round pin was shown above, we show that this technique is adaptable even for such geometries. A silk fibroin coating was deposited on a Ti6Al4V screw (Lincotek Trento S.p.A) as shown in Figure 3b. Figure S2, Supporting Information, shows the SEM images of the unmodified and modified screws confirming the deposition. Coated samples are uniform with a similar surface morphology to the cross-section image shown in Figure 3a. The deposition on a curved surface can lead to a difference of thickness owing to a differential etching mechanism due to variations in height between the plasma nozzle and surface. To avoid this effect, when the sizes of curved parts are bigger in comparison with the diameter of the plasma plume, it is necessary that the plasma torch follows the geometry of the part during its scan. When the diameter

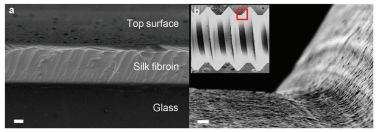

Figure 3. a) SEM image showing the cross-section of deposited silk-fibroin on glass. Scale bar = 1 µm. b) SEM image showing deposited silk fibroin coating of Ti6Al4V screw. Scale bar = 2 µm.

© 2021 The Authors. Advanced Materials Interfaces published by Wiley-VCH GmbH

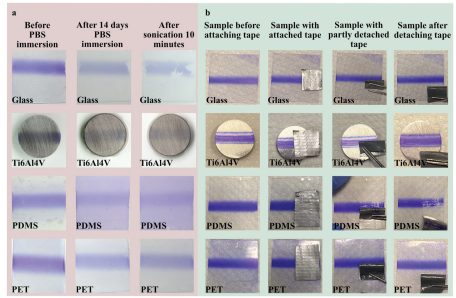

Figure 6. a) Photos of the silk fibroin films observed in buffer solution for 2 weeks at 37 °C following ultrasonication treatment in water. All photos were made in wet condition. b) Photos of the silk fibroin film before and after the peeling test using adhesive tape. Before the test, samples were immersed in a crystal violet solution and dried with nitrogen.

the etching mechanism. This might lead to less micro-delamination regions. PET is less affected by the plasma due to hardness, better wettability, and inability to stretch. These factors reduce delamination regions and enhance adhesion in comparison with PDMS. We assume that, during deposition, the plasma charges both the substrate surface and silk-fibroin aerosol solution, increasing the electrostatic interaction.[36,47] In the meantime, the plasma might induce surface modification by itself. On the glass surface, the plasma results in the formation of OH groups on the surface, arising from the water in the fibroin aerosol, while the presence of nitrogen inserts amide groups on the surface.[48]

On PDMS, the plasma increases the presence of polar groups on the surface, such as SiO_2, Si–OH and Si–CH_2OH, while the nitrogen gives rise to the formation of NH_2 groups.[49–51] In the case of PET, the plasma induces the formation of oxygen functional groups such as hydroxyl and carboxyl groups on the surface;[52] while nitrogen can induce the formation of amide functional groups.[53] Plasma deposition on titanium alloys might increase the thickness of the oxide layer, promoting surface hydration, while also inducing the formation of oxygen functional groups on the top of the surface.[54] All these factors can promote the formation of the covalent bonding between protein and surface, thereby increasing the adhesion strength on these surfaces.

Plasma-assisted deposition of silk fibroin polymer combines the advantages of plasma processes and silk fibroin as a natural polymer. It allows the deposition of uniform and homogeneous silk fibroin films on metals with complex geometry, glass, and flexible materials such as PET and PDMS. It is notable that, on the chosen substrates, the different surface properties and interactions with plasma have a low impact on the conformation of silk fibroin. Plasma deposition provides a controllable and tunable deposition process with linear growth in thickness. Due to the etching process, the roughness of the films is quite high, which can be an advantage for biological applications. Moreover, this atmospheric plasma represents a benign process, characterized by low power and low temperature, but efficient deposition. A minimal change of the protein structure is obtained in comparison to other techniques such as film casting from aqueous solution and β-sheet induction by methanol exposure. Due to the insolubility and flexibility of the deposited silk fibroin films, no post-treatment procedures are needed. The most interesting and promising advantage of this method in flexible applications is the outstanding adhesion between substrate and silk fibroin film. Covalent bonding with enhanced electrostatic interaction provides no delamination after bending of PET and PDMS substrate. The peeling test also shows good adhesion with excellent stability in PBS solution suitable for biomedical applications. These silk fibroin

© 2021 The Authors. Advanced Materials Interfaces published by Wiley-VCH GmbH

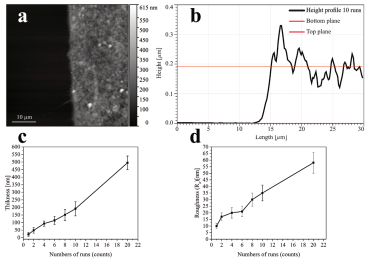

Figure 4. a) AFM image of film edge. Scale bar = 10 µm. b) Height profile across the film edge. c) Thickness dependence of plasma deposited silk fibroin films on the number of runs on the glass substrate (power–10 W, speed–100 mm min^{-1}). d) Roughness dependence of plasma deposited silk fibroin films on the numbers of runs on a glass substrate (power–10 W, speed–100 mm min^{-1}).

of the plasma plume is bigger than the sizes of curved parts, the use of multiple runs can minimize the variation in surface thickness of the coatings.

2.2. Microstructure of the Silk Fibroin Coatings

The microstructure of the deposited fibroin films was characterized using AFM in order to understand the conformation and growth on different substrates as shown in **Figure 4**. The AFM was used to observe the interface of the film with the underlying substrate to observe the film edge and determine film thickness. The thickness obtained from the cross-section was 191 ± 47 nm (Figure 4a,b). The thickness of the plasma deposited silk fibroin on glass substrate increases linearly with the number of runs, confirming LbL deposition (Figure 4c). It may be expected that after deposition of a certain thickness of silk fibroin layer, the plasma plume does not reach the substrate, minimizing etching mechanism and promoting deposition process, which explains the high growth from 190 (10 runs) to 495 nm (20 runs). Standard deviation values are correlated with the surface roughness values (Figure 4d). AFM scans showing the nanoscale surface morphology are presented in Figure S3, Supporting Information, which show almost the same lateral granular sizes in comparison with standard LbL deposition techniques with lateral granular sizes in the order of micrometers. It is worth noticing that while the granular size is the same, the surface roughness (R_a) is much higher, 35 nm ± 6 nm in comparison with 1.34 ± 0.12 nm for stepwise deposition,[34,13] in which silk fibroin solution was obtained by dissolving silk fibroin in LiBr. While, silk films obtained by casting from solution, prepared by dissolving degummed silk in $CaCl_2/H_2O/C_2H_5OH$, also show lower values.[55] Such high values of surface morphology of plasma deposited silk fibroin films can be explained owing to the uneven etching mechanisms occurring during plasma deposition. Figure S3, Supporting Information, shows the surface morphology of the silk films on glass, PDMS, PET, and Ti6Al4V. Glass, PDMS, and PET show almost the same R_a (45 ± 9 nm, 43 ± 10 nm, 41 ± 9 nm) and lower values with respect to the Ti6Al4V, for which R_a is 71 ± 32 nm. Such an increase in roughness can be explained by the higher roughness of bare Ti6Al4V. Moreover, the granular sizes on all substrates are the same, proving that the substrate itself has a low influence on the deposition process. We also assume that silk-fibroin can orient itself on a conductive substrate in the direction of the conductive path. This can be hypothesized owing to the formation of microcavities during polishing, promoting the orientation of silk fibroin (Figure S3d, Supporting Information).

2.3. FTIR Analysis and Structure Reconstruction

Understating the influence of the plasma on the structure of the deposited silk fibroin films is important for tailoring high-impact material functionalization. Different depositions were performed using both nitrogen and compressed air as cooling gases, at power values, ranging from 10 to 25 W. As noted earlier, 10 W is the minimum value at which the plasma is stable and reproducible, while 25 W is the upper limit at which deposition can occur. At higher power, etching processes play a much larger role than deposition processes, perverting film growth.

© 2021 The Authors. Advanced Materials Interfaces published by Wiley-VCH GmbH

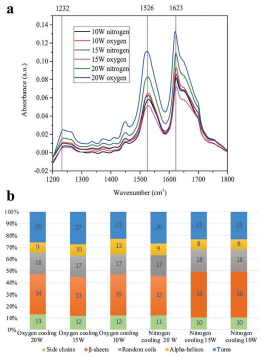

Figure 5. a) ATR-FTIR spectra of a deposited silk-fibroin film. To make film homogenous for the analysis, the following deposition parameters were used: number of runs–16 (3 runs at 100 mm min^{-1}, then 5 runs at 300 mm min^{-1}, and then 8 runs at 500 mm min^{-1}), substrate–glass, distance from the substrate–6 mm. b) Quantitative data of secondary structure of deposited silk fibroin films.

Compressed air was chosen in order to evaluate the changes of silk fibroin structure in an oxygenated environment. With compressed air cooling, oxygen molecules tend to neutralize free electrons from the plasma, making it less effective from a physicochemical point of view. ATR-FTIR measurements were used to understand the structure of the plasma deposited silk-fibroin films. **Figure 5a** shows the amide I absorption band at 1623 cm^{-1}, amide II absorption band at 1526 cm^{-1}, and amide III absorption band at 1232 cm^{-1}. A strong peak at 1623 cm^{-1}, which is a characteristic of antiparallel β-structures, with the shoulder at 1648 cm^{-1} is a common feature of deposition methods.[37,38] In order to evaluate the secondary structure of deposited silk-fibroin films, Fourier self-deconvolution and peak fitting were used (Figure S4, Supporting Information). The area of fitted peaks is correlated with a secondary structure. The data of the relative ratios are reported in Figure 5b and Table S1, Supporting Information. From the analysis, plasma deposited silk-fibroin deposited on glass has a high quantity of β-sheets (32 to 38%), side chains (10 to 13%) and α-helix (8–11%), and a low quantity of random coils (17 to 18%) and turns (23 to 27%).

This minor difference in quantity leads us to hypothesize that changing power and cooling gas have a lower influence on the secondary structure of silk fibroin coating. To determine the effect of the atmospheric plasma on silk fibroin, the secondary structure of the obtained coatings was compared with data on fibroin films previously reported.[37] The plasma coatings exhibit similar content of β-sheets and α-helix, but a lower percentage of random coils compared to silk fibroin films formed by solution casting in polystyrene petridishes without post-treatment (32% β-sheets, 8% α-helix, and 30% random coils). The same films, after methanol annealing, evidenced β-sheets increase to 52%, with a strong reduction of random coils (18%). In these films, the strong reduction of amorphous regions (random coil) is at the base of their stability in water, similar to plasma deposited silk fibroin coatings. We assume that crystalline regions (β-sheets structure), due to their stability, are less affected by plasma treatment.[38–41] It is also evident that plasma can modify and change the structure of the silk protein, inducing conversion of random coils into side chains. In Argon gas, which creates an inert atmosphere in the deposition area, the formation of β-sheets might be induced by the dehydration of the structure.[38] The structure can also be influenced by the substrate, like glass, where β-sheets formation is favored.[42] Thus, depending on the substrate selected, these parameters can be tuned in order to achieve optimal film coatings.

2.4. Adhesion Strength and Stability of the Coatings in Aqueous Environments

The stability and adhesion of the fibroin layer to the underlying substrate is a crucial point in evaluating various deposition techniques for flexible applications. Images of the samples before and after soaking in PBS buffer over 2 weeks are shown in **Figure 6a** and Figure S5, Supporting Information. All samples showed a stable (undissolved) silk fibroin coating. This is presumably due to the high crystallinity of the structure (over 30% β-sheets) and low content of random coils (17–18%).[43] It may be noted that the fading of the blue color of the films is merely due to washing out of the crystal violet solution. We also assume that owing to dehydration and the inert atmosphere of the fabrication process, the deposited films are already very dry, allowing them to be stable in air for a long period of time without any degradation. Meanwhile, we expect that the deposited fibroin will undergo proteolytic degradation, following pathways already described in the literature.[44,45] Plasma deposited films, therefore, showed good adhesion to the underlying surface also after attaching and detaching adhesion tape (Figure 6b). Lower adhesion to the PDMS substrate might be due to low wettability, high stretchability of the material, and plasma behavior on it. PDMS is a soft material that might be more affected by plasma, inducing rougher morphology onto PDMS during deposition, with micro or even nano delamination regions. While immersing the sample in crystal violet aqueous solution, water might pass between the silk fibroin film and the PDMS substrate, reducing adhesion. Changing the cooling gas from nitrogen to compressed air could lead to better adhesion. Firstly, increasing oxygen content in plasma flow might induce better oxidation of the surface and increasing wettability. As noted earlier, oxygen molecules make plasma less effective from a physicochemical point of view, reducing

© 2021 The Authors. Advanced Materials Interfaces published by Wiley-VCH GmbH

Prerequisiti per il corso

1) Analisi 1 (bene) & Analisi 2 (campi vettoriali).
2) Fisica 1.

Programma del corso

1) Elettrostatica.
2) Circuiti elettrici (condensatori e resistenze) .
3) Proprietà e sorgenti del campo magnetico.
4) Induzione elettromagnetica e induttanze.
5) Equazioni di Maxwell.
6) Ottica geometrica e strumenti ottici.
7) Onde meccaniche e nella materia.
8) Onde elettromagnetiche.
9) Interferenza e diffrazione di onde.
10) Polarizzazione della luce.
11) Cenni di fisica relativistica e quantistica (facoltativi per l'esame).

Elettrostatica

1) Forze fra cariche elettriche.
2) Campo elettrico prodotto da distribuzioni di cariche.
3) Legge di Gauss.
4) Potenziale elettrostatico.
5) Lavoro del campo elettrico sulle cariche elettriche.
6) Comportamento di conduttori ed isolanti in campi elettrostatici.
7) Condensatori e accumulo di energia elettrostatica.
8) Tecnologie basate sui fenomeni elettrostatici.

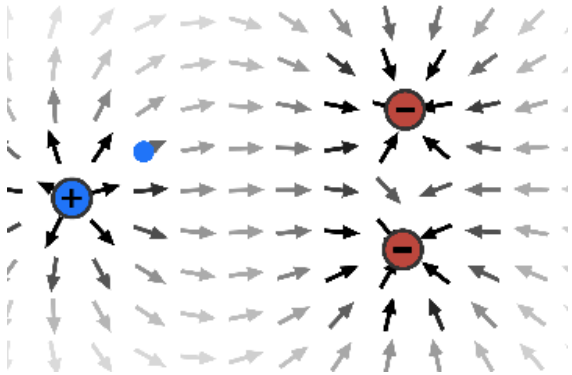

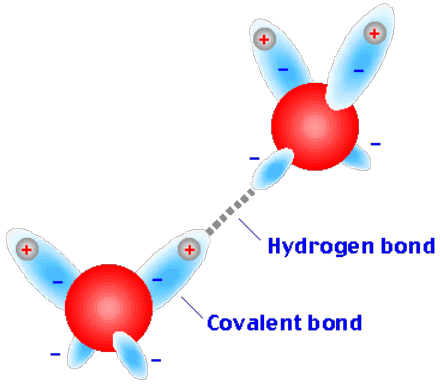

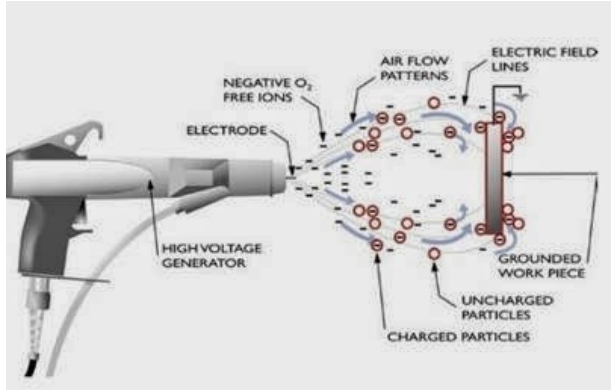

Circuiti elettrici

1) Corrente elettrica.
2) Resistenza elettrica e leggi di Ohm.
3) Circuiti di resistenze: leggi di Kirchhoff.
4) Resistenze collegate a condensatori (circuiti RC).

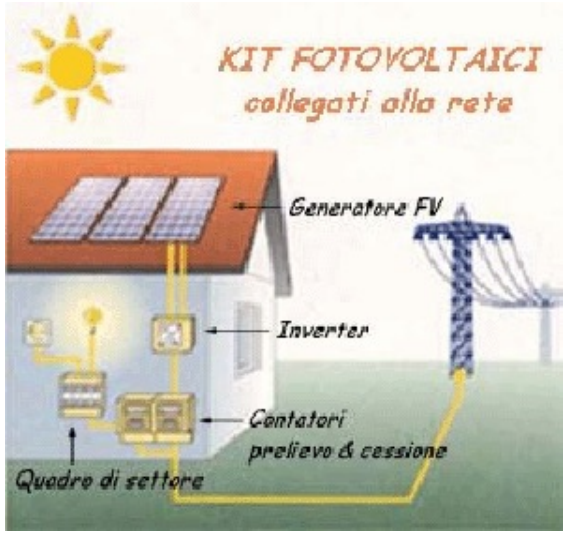

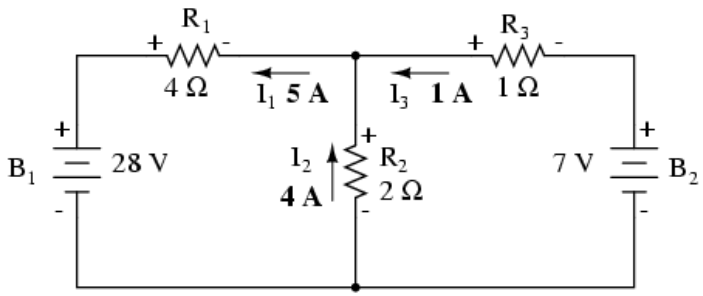

Campo magnetico

1) Proprietà del campo magnetico.
2) Effetti dinamici di un campo magnetico su cariche in moto e circuiti elettrici.
3) Campi magnetici prodotti da correnti elettriche.
4) Legge di Ampére.
5) Magnetismo nella materia.
6) Tecnologie che usano il campo magnetico.

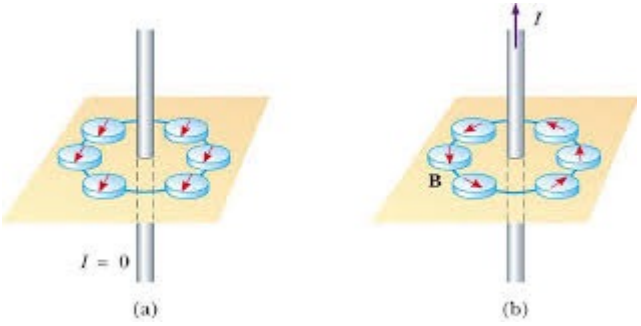

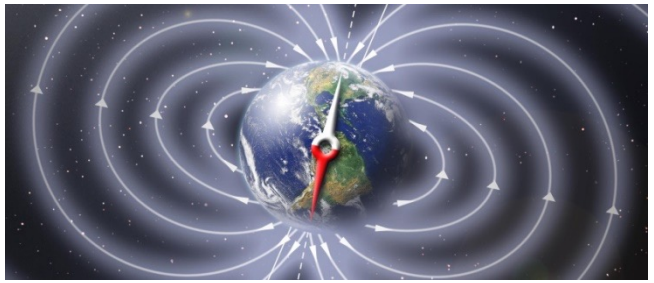

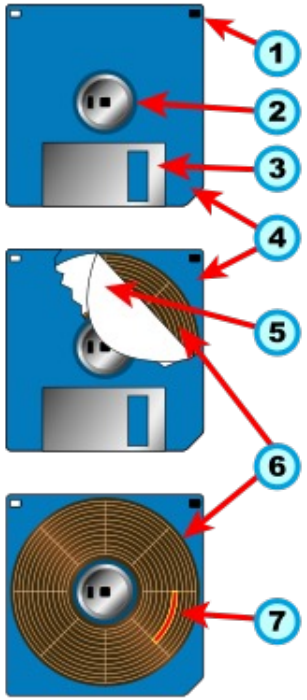

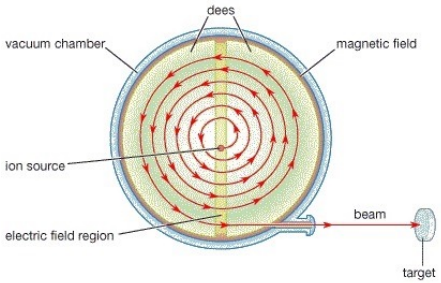

Induzione elettromagnetica

1) Legge di Faraday-Lenz. Forza elettromotrice indotta da una variazione di flusso di un campo magnetico.
2) Induttanza. Energia immagazzinata nel campo magnetico.
3) Collegamenti fra resistenze e induttanze (circuiti RL).
4) Circuiti oscillanti: induttanze collegate a condensatori (circuiti LC).
5) Circuito RLC smorzato e forzato: risonanza.
6) Cenni ai circuiti in corrente alternata.

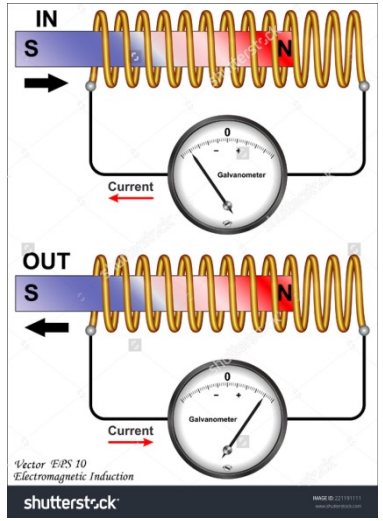

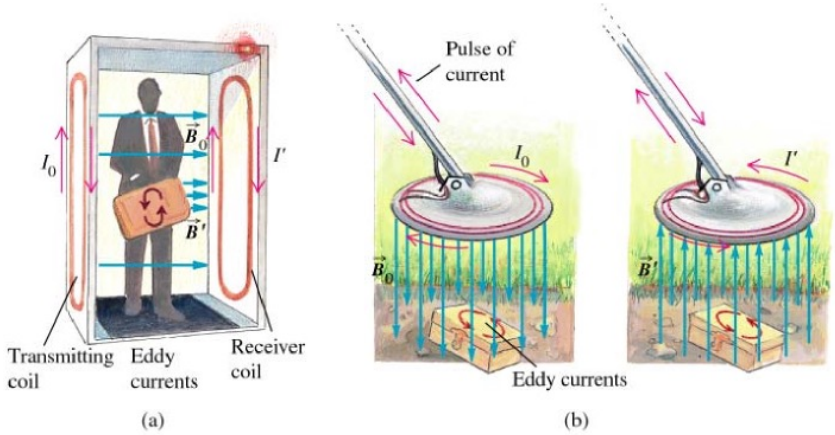

Equazioni di Maxwell

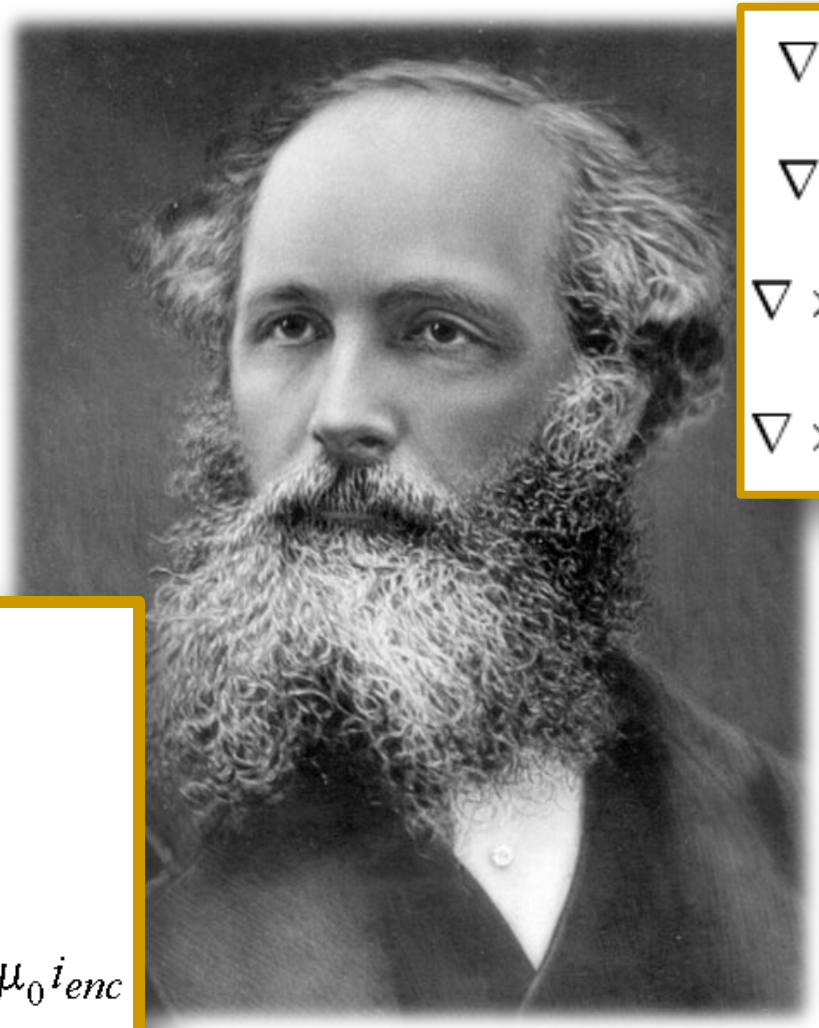

$$\nabla \cdot \mathbf{E} = \frac{\rho}{\varepsilon_0}$$

$$\nabla \cdot \mathbf{B} = 0$$

$$\nabla \times \mathbf{E} = -\frac{\partial \mathbf{B}}{\partial t}$$

$$\nabla \times \mathbf{B} = \mu_0 \mathbf{J} + \mu_0 \varepsilon_0 \frac{\partial \mathbf{E}}{\partial t}$$

$$\oint \mathbf{E} \cdot d\mathbf{A} = \frac{q_{enc}}{\varepsilon_0}$$

$$\oint \mathbf{B} \cdot d\mathbf{A} = 0$$

$$\oint \mathbf{E} \cdot d\mathbf{s} = -\frac{d\Phi_B}{dt}$$

$$\oint \mathbf{B} \cdot d\mathbf{s} = \mu_0 \varepsilon_0 \frac{d\Phi_E}{dt} + \mu_0 i_{enc}$$

Ottica

1) Propagazione a raggi della luce. Immagini reali e virtuali.
2) Legge di riflessione e rifrazione. Indice di rifrazione.
3) Specchi sferici.
4) Diottri sferici.
5) Lenti sottili.
6) Strumenti ottici.

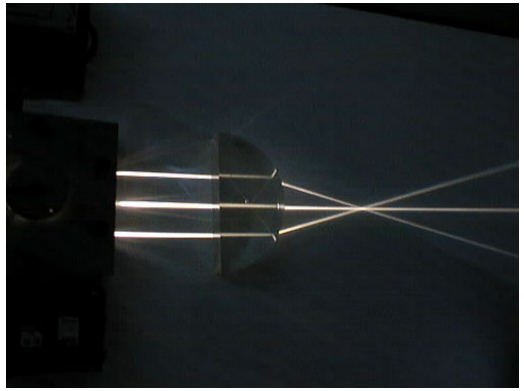

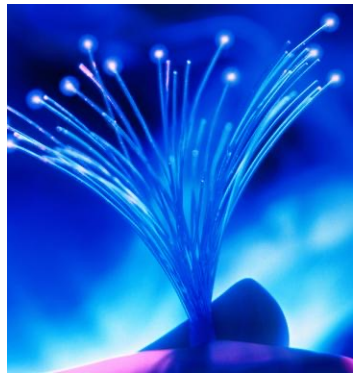

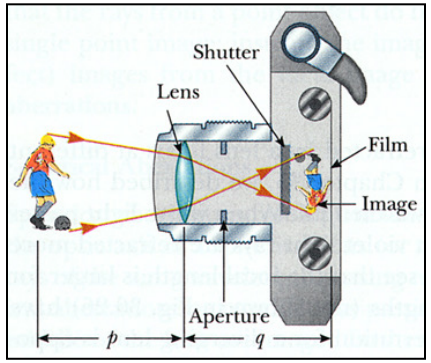

Onde meccaniche

1) Concetto di onda. Equazione generale delle onde.
2) Principio di sovrapposizione.
3) Onde armoniche.
4) Onde meccaniche su una corda e lungo un solido.
5) Onde stazionarie.
6) Onde sonore.
7) Effetto Doppler.

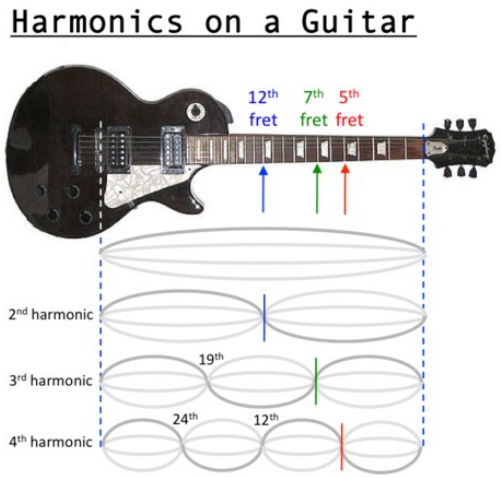

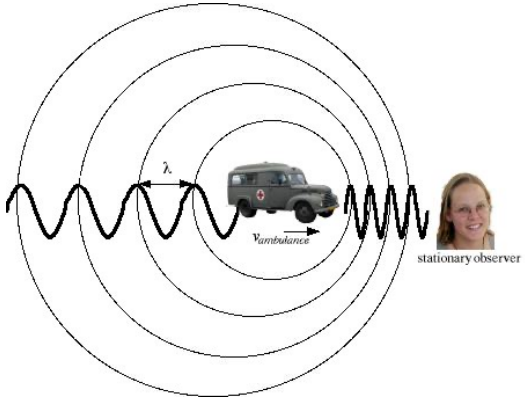

Onde elettromagnetiche

1) Equazione di propagazione del campo elettromagnetico.
2) Proprietà del campo elettromagnetico in un'onda.
3) Energia trasportata da un'onda elettromagnetica.
4) Spettro delle onde elettromagnetiche.
5) Tecnologie basate sulle onde elettromagnetiche.

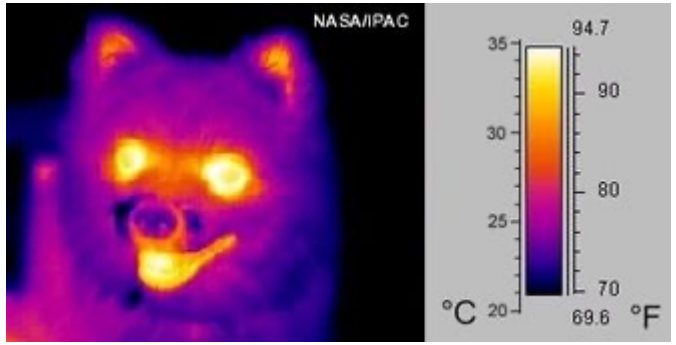

Interferenza e diffrazione

1) Interferenza di due onde coerenti e intensità dell'onda risultante.
2) Interferometro di Young.
3) Interferenza su lamine sottili.
4) Fenomeni di diffrazione.
5) Figura di diffrazione di una fenditura sottile.
6) Interferenza e diffrazione nella tecnologia.

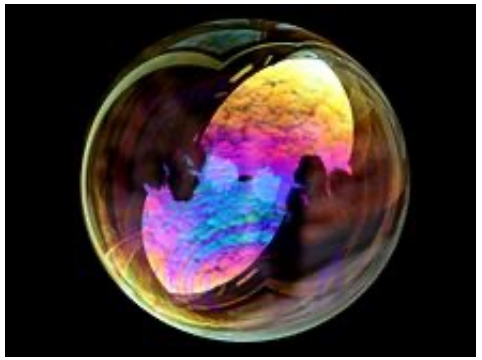

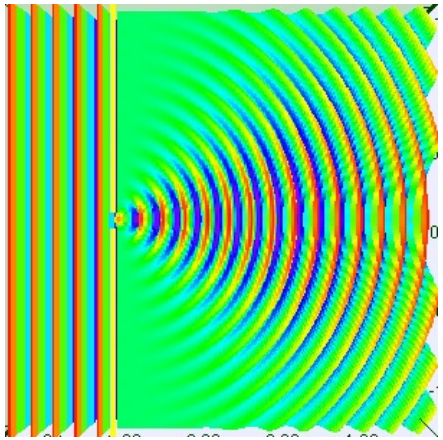

Polarizzazione della luce

1) Polarizzazione di un’onda elettromagnetica.
2) Stati di polarizzazione.
3) Polarizzatori e intensità risultante combinando più polarizzatori.
4) Birifrangenza e analisi degli stati di polarizzazione.

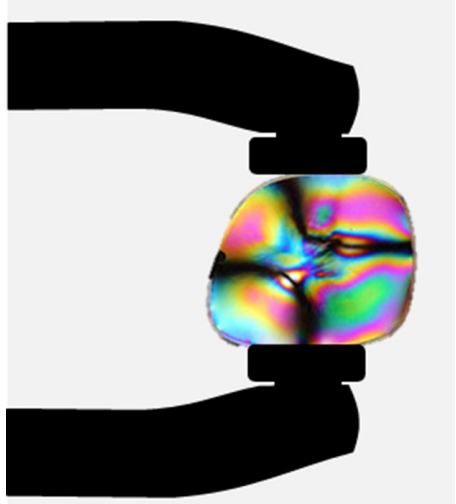

Una testimonianza

Salve prof, sono stato suo studente nel 2013. Dopo aver fatto la magistrale in ingegneria del veicolo e aver lavorato nell'automotive sono finito nel settore dei semiconduttori e lavoro su macchinari che usano la fotolitografia. Ecco adesso dopo anni rimpiango di non aver studiato meglio e di aver preso un misero 23, mi ricordo ancora quando all' orale mi disse una bella bestemmia rimandandomi alla sessione successiva, me la meritavo tutta. Adesso sto rispolverando gli appunti di fisica 2.

Materiale di Studio

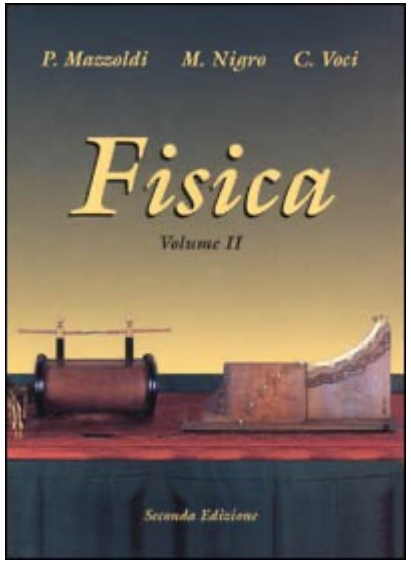

Mazzoldi, Nigro, Voci
Per consultazione
(ma anche Halliday-Resnick; Mencuccini)

Paolo Mazzoldi
1936-2015

Appunti e lucidi del corso

Materiale Aggiuntivo su Moodle

- Slides presentate durante il corso
- Esercizi di autovalutazione
- Esercizi proposti in classe
- Compiti di appelli passati
- Domande di riferimento per l'esame orale
- Lezioni registrate (?)

Formazione sul Rischio in Laboratorio

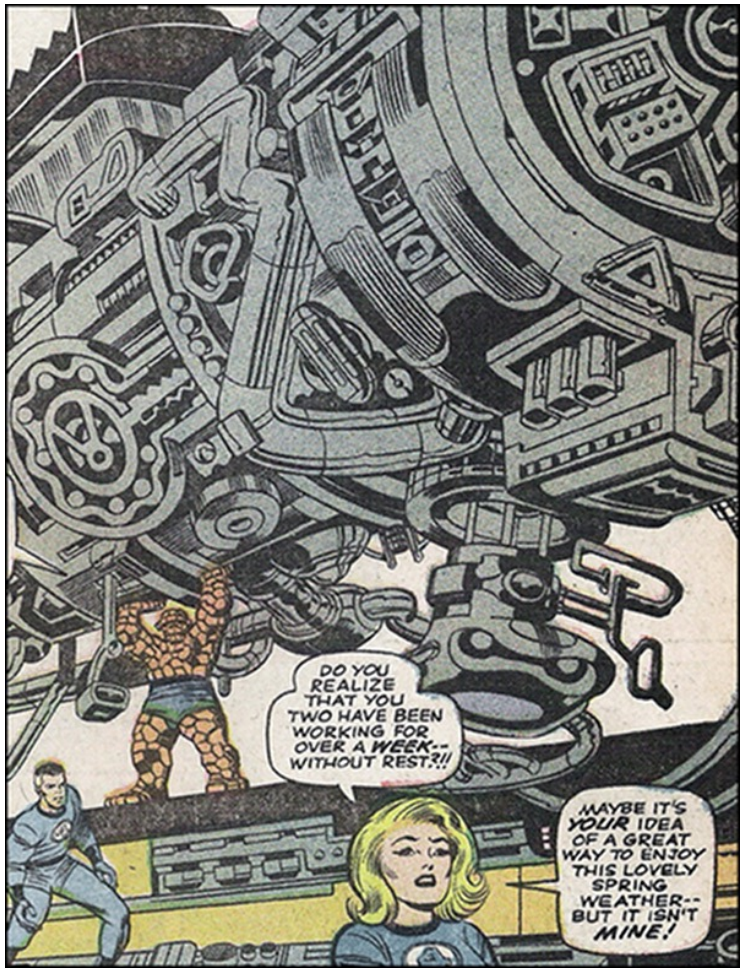

Formazione Specifica - Rischio Medio
Il corso è obbligatorio per frequentare corsi di laboratorio (Laboratorio di Fisica, I semestre del II anno LT Ingegneria Industriale).

Il corso è di 8 ore in presenza, in sessioni con al massimo 35 partecipanti, con obbligo di frequenza di almeno il 90% delle lezioni.

Date e orari:
Mercoledì 27 settembre, 13,30 – 17,30 (4 ore)
Mercoledi 4 ottobre 2023, 13,30 – 17,30 (4 ore)

Aule:
Sessione 1 – Aula A105
Sessione 2 – Aula A110

Leggere il documento caricato su Moodle

Modalità di esame: prova scritta.

- **Prova scritta e orale** (ammessi all'orale con voto ≥ 18).
- 2 scritti parziali (31 ottobre e 19 dicembre) o 1 scritto globale agli appelli ufficiali.
- Con le prove parziali si è ammessi all'orale anche se uno degli scritti ha un punteggio minimo di 15/30 e la media dei due risulta ≥ 18, **ma va fatto l'orale entro febbraio**.
- Niente libri di testo o appunti da consultare durante lo scritto.
- 1° parziale: elettrostatica, circuiti, magnetostatica. 2° parziale: induzione, ottica, onde, interferenza.
- Prova scritta globale: 7 problemi su tutto il programma (due da max 5/30 e cinque da max 4/30).
- Vanno spiegati o indicati i passaggi che portano al risultato finale.
- Uno scritto ha punteggio pieno se è completamente esatto. Il punteggio per ogni esercizio viene decurtato a seconda della gravità degli errori.

Modalità di esame: prova orale

- 3 domande sorteggiate alle quali inizialmente si risponde per iscritto (senza eccessivi dettagli).
- In seguito il docente fa domande per precisare la risposta scritta.
- Non è ammessa l'ignoranza di parti macroargomenti (ottica, onde, magnetismo…) o di argomenti fondamentali (verranno indicati durante il corso).
- Su Moodle verranno indicate gli argomenti che vengono richiesti.
- Verranno caricate anche domande tipo.
- Con molti iscritti l'appello si svolgerà su più giornate. Verrà inviato un calendario dei turni ma sarà possibile cambiare turno secondo le esigenze personali.

Quanto tempo vale lo scritto

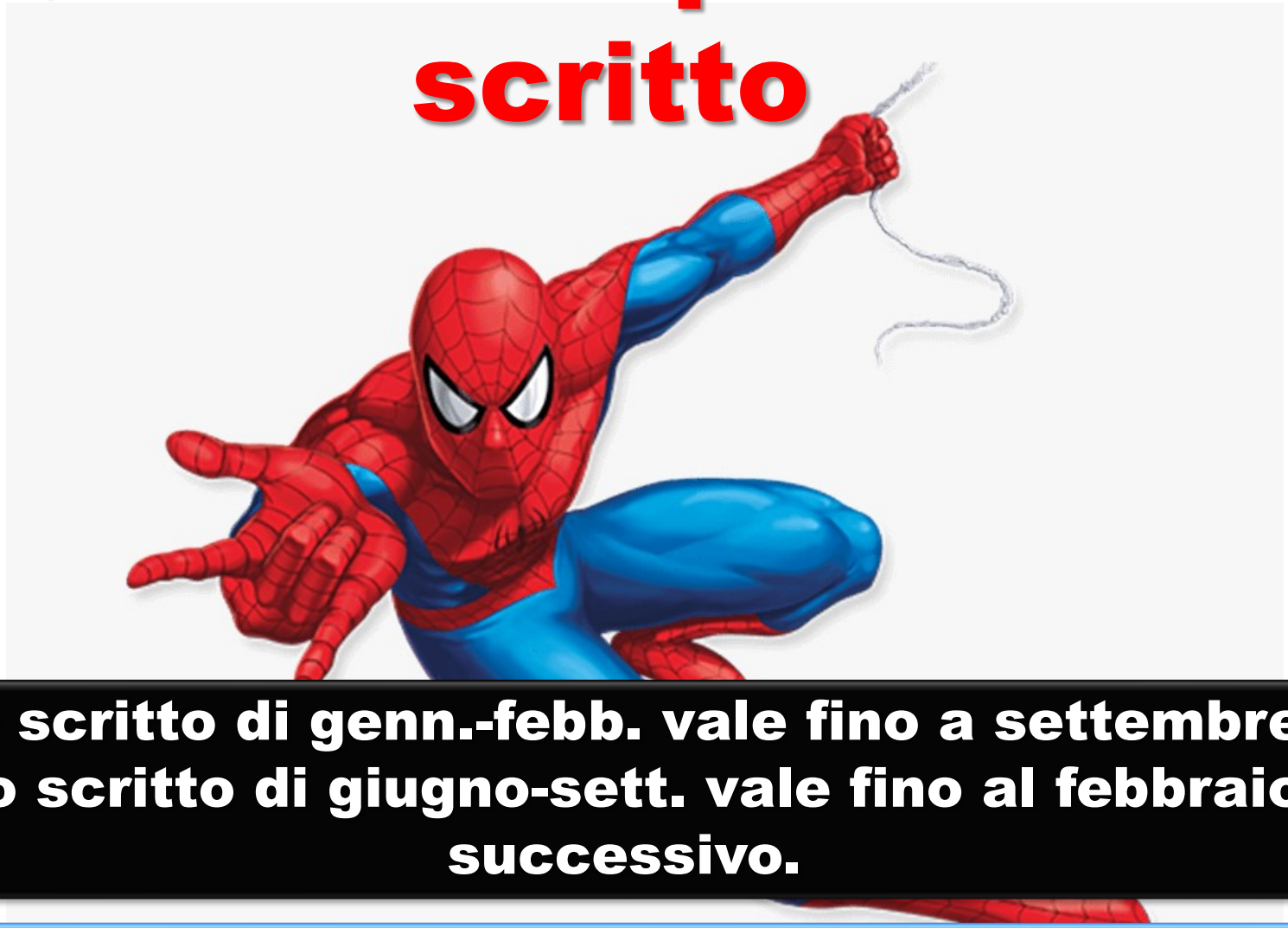

Lo scritto di genn.-febb. vale fino a settembre. Lo scritto di giugno-sett. vale fino al febbraio successivo.

POTETE FARE TUTTI GLI ORALI CHE VOLETE FINCHE' VALE LO SCRITTO.

Avvertenze sul docente

- **NON** è responsabile di ESSE3.
- **NON** fa appelli straordinari.
- **NON** tratta il voto finale.
- **NON** chatta. Al massimo due mail.
- **Riceve su appuntamento fissato via mail**.

Esercitatore

Massimo Cazzanelli

Dipartimento di Ingegneria Industriale (DII)

Massimo. Cazzanelli@unitn.it

Norme di educazione durante la lezione

- Non si mangia.
- Non si chatta col cellulare.
- Sbadigli e conversazioni <u>silenziose</u>.

Consigli per le lezioni

- È fondamentale seguire il corso: il docente indica le cose importanti da sapere usando i termini e le descrizioni che dovete padroneggiare per conoscere la materia.
- Prendere appunti per iscritto. Scrivere mantiene la concentrazione.
- Gli appunti non devono essere un dettato. Scrivete anche le domande che vi sorgono al momento.
- Alla fine della lezione provate a ripetere passaggi e i ragionamenti e se qualcosa non è sufficientemente chiaro chiedete al docente di chiarirvelo.
- Buona pratica sarebbe riguardare le lezioni precedenti in modo da non perdere il filo.

Domande

- Fare domande è importante.
- Sarebbe meglio farle durante la spiegazione perché possono essere utili per gli altri.
- Se siete troppo timidi potete fare domande anonime scritte dopo ogni ora o via mail.

«Strategie» per superare l’esame

❖ Studente prima dell’esame.

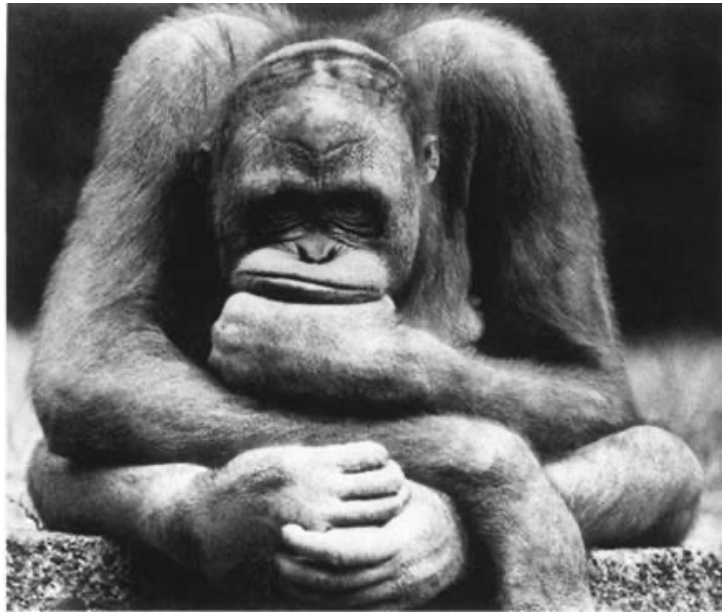

❖ Studente durante l’esame.

Per prepararsi allo scritto

- L'unico modo per prepararsi allo scritto di fisica è risolvere tanti problemi, meglio se da soli.
- (Ri)fare i problemi svolti in classe da soli senza guardare i passaggi svolti dal docente.
- Fare gli esercizi di autovalutazione proposti dal docente.
- Svolgere esercizi di testi di Fisica 2 per scienze/ingegneria eventualmente consigliati dal docente.
- Chiarirsi i dubbi durante l'anno (molto) prima di arrivare all'appello.

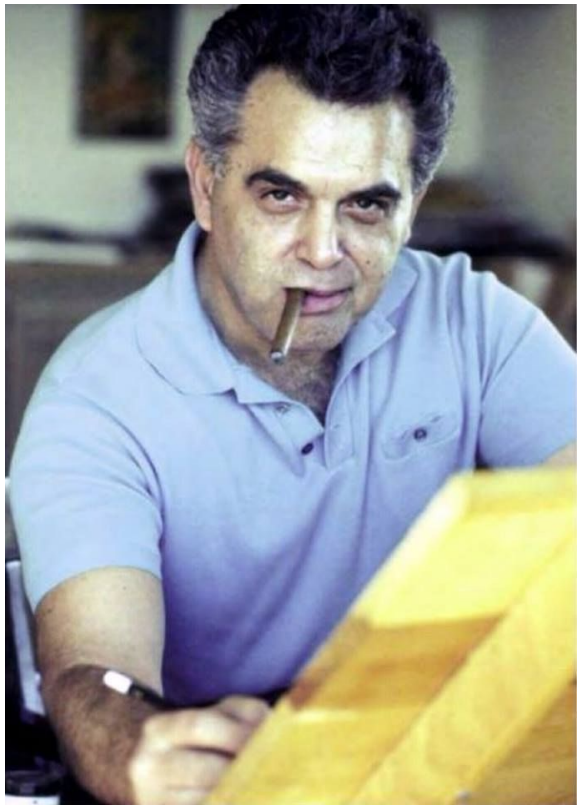

Jack Kirby

Per prepararsi all'orale

- Fatevi una lista di possibili domande.
- Preparate una risposta come se fosse una lezione a persone impreparate e disinteressate.
- Se vi accorgete che un passaggio o un concetto non escono chiari consultate un testo o gli appunti.
- La ripetizione dà un senso di sicurezza e attenua l'ansia da prestazione.

Learning Pyramid

(National Training Laboratories, Bethel, Maine)

α	Α	Beta
β	Β	Alfa
γ	Γ	Lambda
δ	Δ	delta
ε	Ε	Lambda
ζ	Ζ	Lambda
η	Η	Lambda
θ	Θ	Lambda

ι	Ι	Lambda
κ	Κ	Lambda
λ	Λ	Gamma
μ	Μ	Lambda
ν	Ν	Lambda
ξ	Ξ	Fcxhjki
ο	Ο	Lambda
π	Π	Lambda

ρ	Ρ	Lambda
σ	Σ	Lambda
τ	Τ	Lambda
υ	Υ	Lambda
φ	Φ	Lambda
χ	Χ	????
ψ	Ψ	Lambda
ω	Ω	Lambda

IN BOCCA AL LUPO